An Experimental and Numerical Analysis of Effects Induced by Moving Bodies in Free Surface Water.

F. Kerger[1,2], S. Detrembleur[1], P. Archambeau[1], S. Erpicum[1], B.J. Dewals[1,2] and M. Pirotton [1]
[1]*Laboratory of Applied Hydrodynamics and Hydraulic Constructions, Institute of Civil Engineering, ArGEnCO Department, Liège University, Ch. Des Chevreuils 1, B52/3+1, B-4000 Liege, Belgium, fkerger@ulg.ac.be*
[2]*Belgian Fund for Scientific Research F.R.S-FNRS*

ABSTRACT: Dynamics of free surface flow induced by a partially or totally submerged moving body generates efforts on it. In the design process of moving hydraulic structures and their maneuvering system, one needs to quantify the pressure field acting on it. A fundamental example of such phenomenon, namely the vertical uplift of a submerged horizontal rigid sheet, is hereafter experimentally analyzed. The present study includes the description of the experimental apparatus built in the HACH laboratory and the description of the rigorous experimental procedure used. The purpose of the analysis is to identify the fundamental hydrodynamic mechanisms involved. Such identification is indeed a prerequisite to develop an accurate numerical algorithm. Finally, it is shown that six fundamental mechanisms account for the whole pressure field around the panel.

1. INTRODUCTION

The dynamics of free surface flow induced by the essentially vertical motion of a submerged body is a complex phenomenon, still today quite difficult to foresee. In particular, it remains challenging to predict the efforts generated by the flow on the body. Phenomenon intricacy results from the underlying relationship between the pressure field surrounding the moving body and the velocity field resulting from its movement. Indeed, even if the pressure field arises from the flow, one must conceive of this field as the driving force of the flow.

From a civil engineering point of view, several hydraulic structures may be assigned to this category of phenomena. In particular, flap gate movement, sealing the lock by coming from a chamber at the bottom of the lock foundation raft, is an evocative example. This practical application highlights that civil engineers need to be able to predict the efforts generated by the flow and the induced flow dynamics.

To the author's knowledge, neither general theory nor design method has been proposed in literature. Traditionally, the design of this kind of structure is performed by creating an instrumented physical scale model in laboratory. Therefore, the actual hydraulic structure is designed by extrapolating the experimental data using similarity laws. This method has been successfully applied to a wide range of application [11]. However, build the scale model turns out to be expensive and the optimisation of shapes appears difficult to achieve. For a few practical applications, design table, expressed in terms of non-dimensional parameters [12], are available in the literature. Of course, such tables are purely descriptive and do not give any information about the hydraulic mechanisms.

In a similar manner, the experimental analysis of flap gate motion conducted by Canor [3] has shown the complex flow features involved. He concludes that many phenomena appearing during the uplifting of the gate are still poorly understood. In addition, he shows that relations given in the literature about ship propulsion are not applicable to a vertical movement.

In the last decades, c*omputational fluid dynamics* has been providing an approach of increasing efficiency to design hydraulic structures. Used on its own or combined with a physical model, numerical simulation permits to avoid extensive and expensive optimization on a scale model [6]. However, developing such software is computationally difficult because it is needed to solve the incompressible Navier-Stokes equations in the vertical plane and track the free-surface in parallel [4]. In particular, such a development requires a good understanding of the phenomena involved in the simulated application.

Therefore, authors propose in this study to focus on a more fundamental and theoretical case, namely the vertical uplifting of a metallic rigid sheet from the pool bottom up to the free surface of the still water. This simplification leads to a better identification of the basic phenomena arising during the translation. Experimental results are then exploited to improve the overall understanding of moving bodies in free surface water and to support the development of a numerical tool of simulation [4] with experimental results. The new algorithm is a module of the modelling system *WOLF* developed within the

Laboratory of Applied Hydrodynamics and Hydraulic Constructions of the University of Liege.

This paper is organized as follows. Section 2 details the apparatus and the procedure of the experiments performed at the HACH laboratory. Section 3 exposes results of the campaign and a new model for interpretation. Experimental results are compared with the numerical simulation of an ideal case in section 4.

2. ORIGINAL EXPERIMENTS

2.1. Experimental apparatus

The experimental apparatus is composed of a 10m by 2m pool in sealed masonry based on a concrete slab. This length ensures that perturbations of the measures by the reflected free-surface waves would be avoided in the majority of the experiments. In addition, a honeycombed insulator placed at both ends of the pool lessens the intensity of their reflection. Previous attempts [3] have demonstrated that the pool is wide enough to prevent wall effects in the measurement area. Visualisation of the flow is permitted through a Plexiglas wall which replaces the masonry in the centre part of the pool (Figure 1).

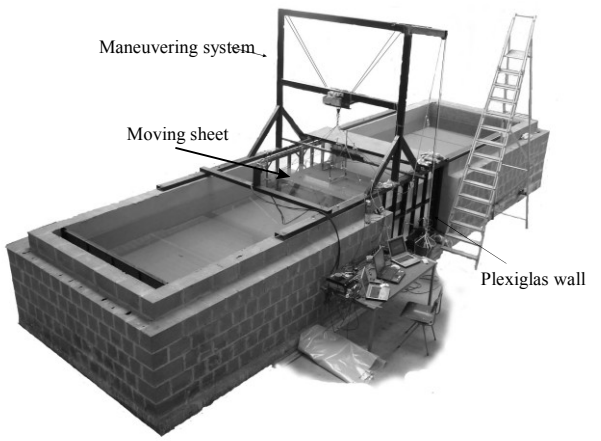

Figure 1 : Experimental apparatus

The rigid horizontal sheet consists of an aluminium orthotropic structure stuck between two Plexiglas panels (Figure 2). During the experiments, hollows in the plate are filled with water and allow us to incorporate pressure gauges. Finally, the unit is 2m long, 0.76m wide and 0.16m thick. The submerged weight is 64kg.

Moving the rigid sheet is achieved by a system of ropes and pulleys (Figure 3). Actually, a frame of steel beams is placed above the pool. Pulleys are fastened to it and hold on a metallic rope linking the sheet to the manoeuvring system. Thanks to this device, the force needed to move the panel is divided by a factor ranging from 3 to 4.

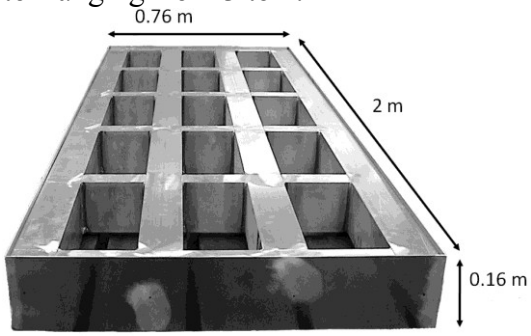

Figure 2 : Aluminum rigid sheet (Plexiglas sheets are missing)

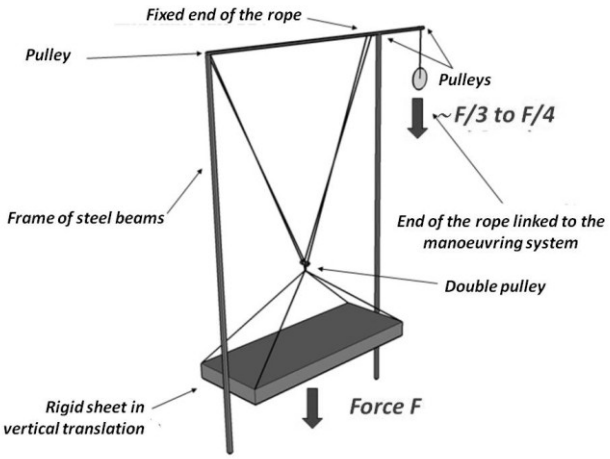

Figure 3 : Diagram of the actionning system

Two manoeuvring systems have been used during the experimental campaign. The first one is an adjustable counterweight, which has the major advantages to allow a highly repeatability of trials and to appraise the overall power provided to the sheet. The second one is a crank which moves the panel at a constant speed.

2.2. Measurement system

The measurement system includes at first five pressure gauges (KELLER series 41 capacitive transmitters). The capsule in this transmitter is a KAVLICO capacitive ceramic pressure element, which is enclosed in a sealed stainless steel housing with the diaphragm protected by a gold layer. An O-ring seals the sensing diaphragm to the housing. Manufacturer assures an accuracy of ± 1mm H_20.

On the one hand, tree of these pressure gauges are fastened onto the central line of the horizontal panel, in parallel to its small side (Figure 4). They are alternatively oriented towards the upper side and the lower side of the plate. On the other hand, two of them are held on 20mm below the free surface and

exactly above the two former ones. They provide the temporal evolution of the free surface elevation.

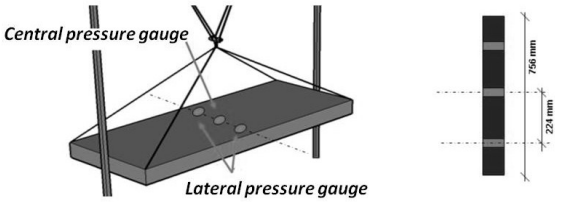

Figure 4 : Position of pressure gauges on the rigid sheet (Lateral pressure gauges are symmetrical)

In addition, the exact position of the rigid sheet is measured by using a potentiometer (Rheostats Bourns 3590S). The potentiometer is fastened to the shaft of a pulley (Figure 5). A rope linked to the moving rigid panel is coiled around this pulley. By this way, the translation of the rigid sheet entails the rotation of the pulley. Hence, the exact position of the panel can be derived from the measured voltage, granted that the relation between the position of the sheet and the voltage has been previously established.

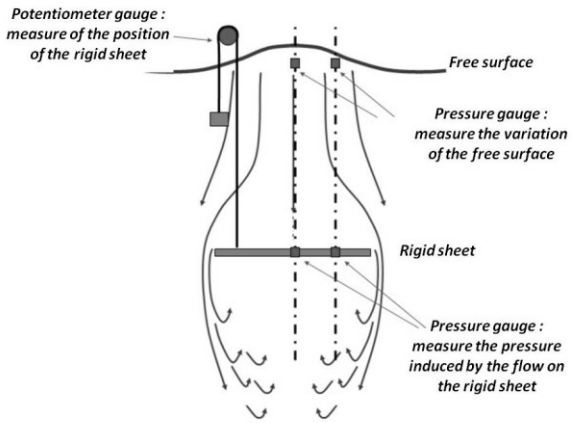

Figure 5 : Complete measurement system

2.3. Experimental campaign

The overall experimental campaign lead within the Laboratory of Applied Hydrodynamics and Hydraulic Constructions (HACH) of the University of Liege involved the following trials:

- two sets of 15 identical trials in which the rigid sheet motion is controlled by an adjustable counterweight (20kg and 30kg) ;
- one set of 25 trials in which the rigid sheet velocity is kept constant along the trial (various steady velocities from 80mm/s to 10 mm/s) ;
- two sets of 3 trials in which the rigid sheet course is shortened (160mm) and performed successively far from the free surface and close to it. These sets aim at identifying the specific influence of the free-surface.

2.4. Experimental procedure

This paragraph exposes the full course of the experiment from the setting of the initial conditions up to the data processing. First of all, in order to assure that the state of the pool would be identical at the beginning of each trial, the rigid sheet is accurately positioned thanks to the pressure gauges.

As soon as the water is not any more in motion, the manoeuvring system is triggered off by discharging the counterweight hanged aloft or by rotating the crank. As a result, the rigid sheet, kept horizontal, moves from the bottom of the pool up to the free surface. During the translation, the measurement system records the temporal evolution of

- the pressure at a central point of the sheet on its upper and lower sides,
- the pressure at a lateral point of the sheet on its upper and lower sides,
- the free-surface elevation directly above the central pressure gauge,
- the free-surface elevation directly above the lateral pressure gauge,
- the position (depth) of the rigid sheet in the water.

Collected primary data are then processed in order to give average values of the parameters for several similar trials and their corresponding confidence interval Δ. This one is given by the classical equation:

$$\Delta = +t^{n} \qquad (1)$$

where $\alpha = 1- 2\gamma$ is the wished level of confidence, N is the number of measures, σ is the unbiased estimator of the variance, and t_{γ}^{n-} is the value of Student distribution, with n-1 degrees of freedom corresponding to the 1- γ probability. The Confidence Interval (IC) chosen in this paper is $\alpha = 95$ %. All charts of the present paper are thus given with the correspondent IC.

Subsequently, statistically processed measured pressures are broken down into several contributions so that all the relevant information may be extracted from the measured data (Figure 6). By this process, the *drag pressure* is defined as the hydrodynamic pressure resulting from the fluid motion augmented by the free surface variation above the rigid sheet (for pressures measured on the lower side of the sheet, this

last contribution is clearly zero). Physically, it consists of excluding the *hydrostatic component* from the measured pressure and keeping only the *hydrodynamic component*. Authors insist here on the fundamental feature of this parameter: characterizing the behavior and identifying factors influencing the drag pressure is the core of the present study.

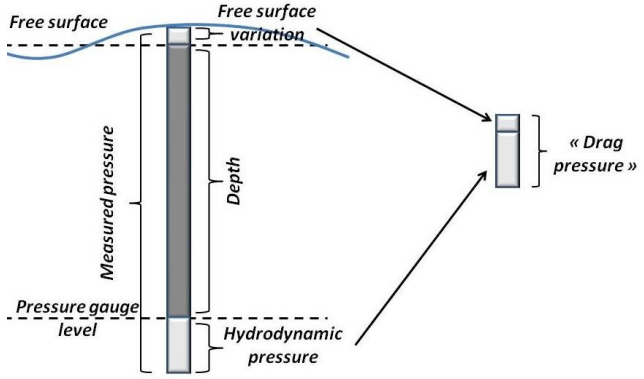

Figure 6 : Definition of the "drag pressure"

3. DIMENSIONAL ANALYSIS

3.1. Hydrodynamics

Application of the Vaschy-Buckingham theorem on the current experiment (see [9]) permits the identification of the Pressure Coefficient

$$C_p = \frac{p}{\rho} = \left(\frac{a}{g}, \frac{x}{l}, \mathrm{Fr}_s, \mathrm{Re}_s \right) \quad (2)$$

where $\mathrm{Fr}_s = \frac{v_s}{\sqrt{g h_s}}$ is the sheet Froude number, $\mathrm{Re}_s = \frac{v_s l}{\nu}$ is the sheet Reynolds number, $a\left[ms^{-2}\right]$ is the sheet acceleration, $g\left[ms^{-2}\right]$ is the gravity acceleration, $x\ m$ is the position on the sheet, $l\ m$ is the sheet width, $v_s\left[ms^{-1}\right]$ is the sheet velocity, $h_s\ m$ is the sheet depth for the upper face or the length between the sheet and the bottom of pool for the lower face, $\rho\left[kg\,m^{-3}\right]$ is the water density, $\mu\left[kg\,m^{-1}\,s^{-1}\right]$ is the water viscosity.

3.2. Aerodynamics

In contrast, the pressure coefficient for a moving body in air (aerodynamics) is given in [2] :

$$C_p = \frac{p}{\rho} = \left(\frac{x}{l}, \mathrm{Re}_s \right) \quad (3)$$

In this case, the distribution of C_p is illustrated on Figure 7. Accordingly, the pressure coefficient for the upper face is comprised between 0 and 1 according to the position on the sheet and its value is equal to -1 everywhere on the lower face.

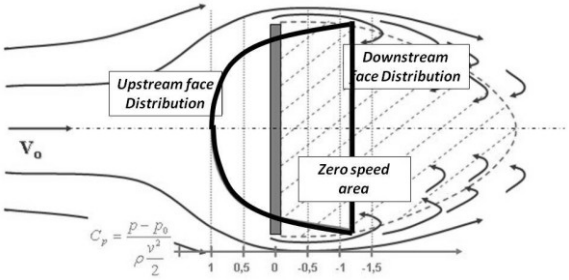

Figure 7 : Pressure coefficient for aerodynamic flow [2]

As pointed in [2], three mechanisms account for the distribution given in Figure 7 :

First, part of the pressure field around the body originates in the pressure decrease induced by the increase of the fluid velocity module

. This mechanism is well-described by the Bernoulli equation :

$$p = \frac{1}{2} v \quad (4)$$

Second, a negative pressure appears behind the rigid sheet in translation due to the flow separation at the sharp ends of the panel.

Third, the natural viscosity of water has a slight contribution to the creation of drag pressure around a moving body.

3.3. Comparison

Comparison between (2) and (3) shows clearly that the pressure coefficient in Hydrodynamics depends not only on the Reynolds number and the position on the body, but also on the Froude number and on the acceleration. This is the main point of the paper. So, the only mechanisms involved in aerodynamics flow cannot account for the whole drag pressure created in a free surface flow. Further mechanisms have to be identified. The question remains which ones?

We aim hereafter at identifying these fundamental hydrodynamic mechanisms. Such identification is indeed a prerequisite to develop an accurate numerical algorithm for the simulation of the flow induced by a vertical moving body. Indeed, all phenomena involved have to be described in sufficient details by the set of equations and the boundary conditions.

4. RESULTS AND INTERPRETATION

4.1. Constant velocity trial - Experimental results

First trial is a vertical translation at a velocity of 95mm/s. Figure 8 shows the velocity and acceleration of the sheet during the translation. Three distinct stages of the motion are observed:

- Stage 1 - Acceleration from zero velocity to the maximum velocity of 95mm/s
- Stage 2 - Translation at constant velocity.
- Stage 3 - Deceleration down to zero velocity.

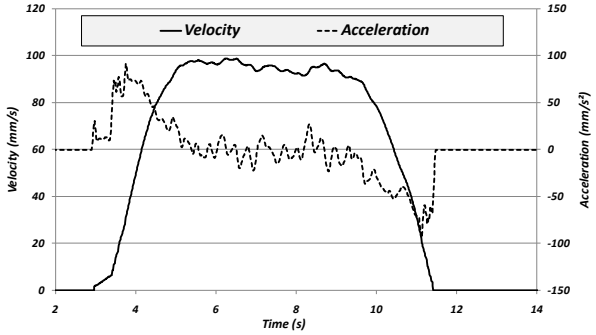

Figure 8 : Velocity and acceleration of the rigid sheet

The evolution of the free surface height as a function of the water depth corresponding to the rigid sheet is shown on Figure 9. The two curves show a sudden but small increase of the free surface level during the initial acceleration and a sharp decrease during the final deceleration. In-between these peaks, the free surface levels off. It suggests that the positive and negative acceleration stages are responsible for a wider extent of the free surface variation than the translation stage. What is more, it seems the impact of the translation varies with the water depth. For deepest water, the variation of the free surface induced by the moving sheet remains faint. In contrast, the free surface oscillation expands substantially while the rigid sheet is ascending and reaches its maximum as the panel surfaces.

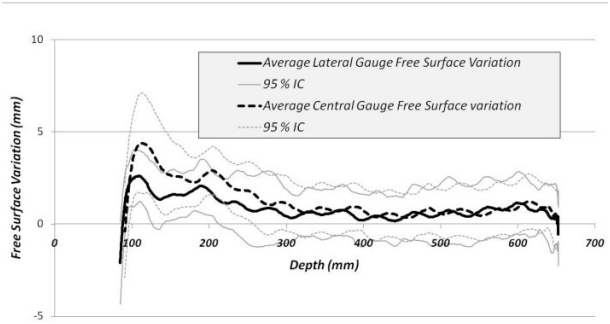

Figure 9 : Free surface evolution (the chart must be read from the right – sheet at the bottom of the pool – to the left – sheet close to the free surface).

Figure 10 and Figure 11 below present the temporal evolution of the drag pressure (as defined in section 2.4) all along the vertical translation of the rigid sheet. A qualitative analyse of the curve related to the upper face shows a sudden increase during the acceleration stage up to a positive and nearly constant value during the translation stage. The deceleration stage comes with a sharp decrease of the drag pressure. For the lower face, the acceleration stage is characterized by a negative peak of pressure. The translation stage appears to be very changeable with a small bias toward negative pressure. Comparison between the values at the central and at the lateral gauges highlights a similarity of behaviour. Still, consistent differences are noted, especially as the panel reaches the free surface. The charts indicate indeed that drag pressures grow stronger at central gauges.

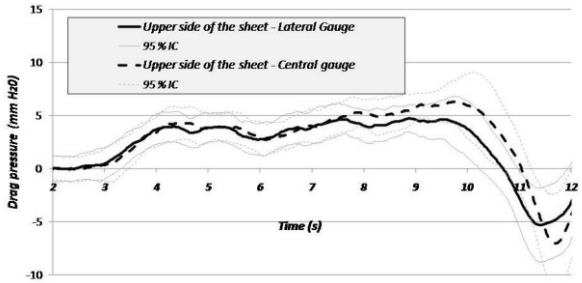

Figure 10 : Drag pressure evolution for the upper face

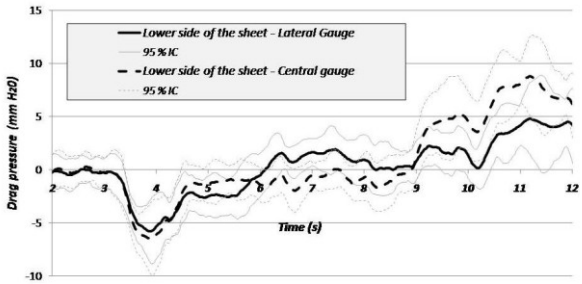

Figure 11 : Drag pressure evolution for the lower face

In Figure 10 and Figure 11, pressure returns progressively to zero after a few minutes. Charts in this paper don't show this stabilization phase of the free surface as it contains no relevant information.

4.2. Controlled power trial - Experimental results

Second trial is a vertical translation with a fixed counterweight of 20kg. So, the energy provided to the panel is controlled. Figure 12 gives the velocity and acceleration of the sheet along the translation. Two distinct stages of the motion are observed:

- stage 1 - Acceleration from zero velocity to the maximum velocity of 160mm/s.
- stage 2 - Deceleration down to zero velocity.

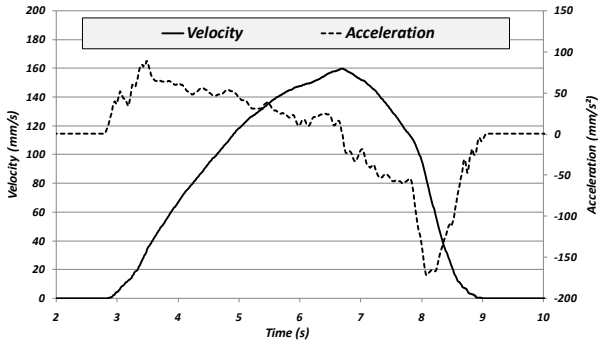

Figure 12 : Velocity and acceleration of the rigid sheet

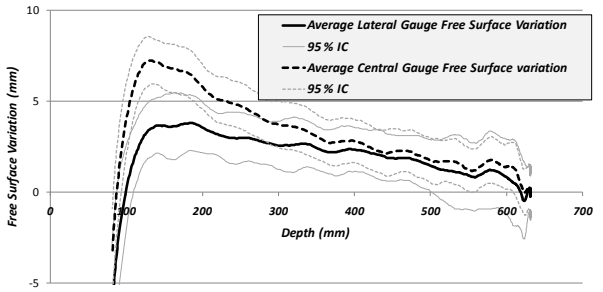

Figure 13 : Free surface evolution (the chart must be read from the right – sheet at the bottom of the pool – to the left – sheet close to the free surface).

The evolution of the free surface height as a function of the water depth corresponding to the rigid sheet is shown on Figure 13. The two curves show a sudden but small increase of the free surface level during the initial acceleration and a sharp decrease during the final deceleration. In-between these peaks, the free surface has been rising steadily. As the water level is still rising when the acceleration begins to decrease, we deduct that the impact of the translation varies considerably with the water depth.

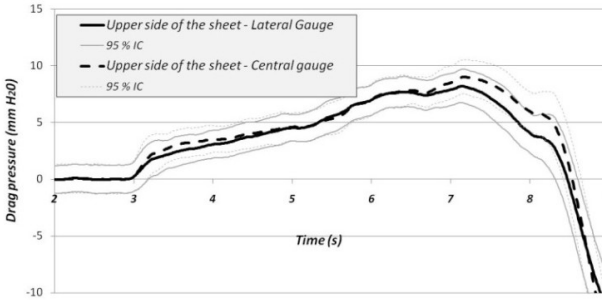

Figure 14 : Drag pressure evolution for the upper face

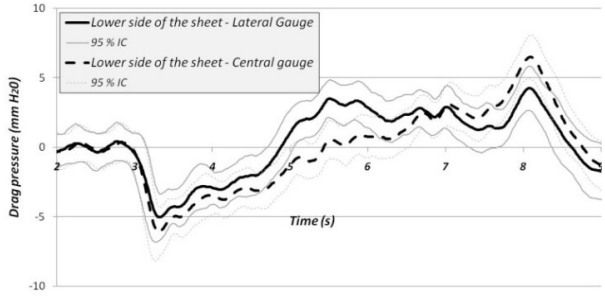

Figure 15 : Drag pressure evolution for the lower face

Figure 14 and Figure 15 illustrate the temporal evolution of the drag pressure all along the vertical translation of the panel. A qualitative analyse of the curve related to the upper face shows a small increase during the acceleration, followed by a continuous rising as long as the speed is increasing. The deceleration stage comes with a sharp decrease of the drag pressure. For the lower face, the acceleration stage is characterized by a negative peak of pressure. The deceleration stage comes with a positive peak of pressure. In-between, the pressure has been increasing steadily. Comparison between the values at the central and at the lateral gauges highlights a similarity of behaviour. Still, consistent differences are noted, especially as the panel is reaching the free surface. The charts indicate indeed that drag pressures grow stronger at central gauges

4.3. Additional experiments

Additional experiments have been performed at various constant velocities and with various counterweights. Similar results have been found. Complete analysis of experimental records are presented in [9]. Measured Cp are also critically analyzed. It is shown that identifying contribution of non-dimensional parameters is quite impossible in Cp coefficient.

4.4. Interpretation

For a constant velocity of 95mm/s, the hydrodynamic pressure expected in aerodynamics (Figure 7) at the central gauge is p/ρ ; = m H_2O If we compare the values given in paragraph 4.1 and 4.2 with the former value, it is clear that further mechanisms have to be identified in addition to the three mechanisms outlined in paragraph 3.2. Based on the theoretical investigations and experimental results given above, authors propose three additional mechanisms.

First, part of the hydrodynamic load provided to the panel by the maneuvering system is consumed to prevail fluid inertia. For a sheet moving at constant velocity , Bernoulli equation can be written

$$\frac{d}{ds}\left(\frac{U}{g} \quad \frac{p}{\rho} \quad z \right) \quad \frac{\partial U}{g \quad t} \qquad (5)$$

where $U\left[ms \right]$ is the fluid velocity, z m is the height and s m is a curvilinear abscise in the direction of the flow. The term of the right side of the

equation (time derivative) accounts for the fluid inertia. As long as the fluid velocity is increasing, this term reinforce the positive pressure on the upper face of the panel and increases the negative pressure on the lower face. In [9], it is rigorously demonstrated that the inertia term is inversely proportional to the square of the panel depth (which is defined as the distance between the free surface and the upper face of the panel). This mechanism is therefore negligible far away from the free surface, as in aerodynamics, and tends asymptotically towards infinity when the rigid sheet surfaces.

Second, as water and panel have close specific weight, they exchange mass momentum during the acceleration and deceleration of the rigid sheet. Under the assumption of a perfect fluid and an irrotational flow, the force exchanged $\Delta F \ \ N$ is proportional to the acceleration $a\left[{}^{m}{}_{s}\right]$ of the panel. The concept of added mass $M_a \ \ kg$ is then introduced in [10] and applicable here :

$$\Delta F = M_a a \qquad M_a \div M_{body} \tag{6}$$

where $M_{body} \ \ kg$ is the mass of the moving body.

Third, a significant part of the hydrodynamic load provided to the panel is consumed by propagation of free surface waves. The free surface waves are created to equilibrate the pressure increase induced to prevail the fluid inertia. Indeed, according to (5), the fluid inertia creates a pressure increase of

$$\Delta p = -\frac{1}{g}\frac{\partial U}{\partial t} \tag{7}$$

below the free surface. The free surface level is however fixed by the local equilibrium of pressure $p_{atmospheric} + \_ = \_\_\_\_$ where p_s is the contribution of the surface stresses. Then, an increase of the water level is necessary to equilibrate the pressure increase (7).

5. NUMERICAL INVESTIGATION

The HACH has been lately developing a new algorithm for the simulation of quasi-vertical free-surface flow. The resolution of the Navier-Stokes equations is carried out on the basis of the well-known finite volume method applied to a regular grid composed of squared meshes. The software solves the Navier-Stokes equations in a vertical plan in two separate steps of calculation (projection method). In the first one, velocity field is approximated by resolving the momentum equation. In the second stage, the Poisson equation for the pressure is solved in order to force the fluid incompressibility. On the basis of the resulting pressure field, the approximate velocity field previously established is corrected to obtain the final velocity field in the whole domain. An outline of the algorithm is introduced in [4].

The herein described model constitutes a part of the modeling system "WOLF", developed at the University of Liege. WOLF includes a set of complementary and interconnected modules for simulating free surface flows: process-oriented hydrology, 1D & 2D hydrodynamics, sediment [5] or pollutant transport, air entrainment, as well as an optimization tool based on Genetic Algorithms [7]. Other functionalities of WOLF 2D include the use of moment of momentum equations [5], the application of the cut-cell method [8], as well as computations considering vertical curvature effects by means of curvilinear coordinates in the vertical plane [6]. A user-friendly GIS interface, entirely designed and implemented by the authors [1], makes the pre- and post-processing operations very convenient.

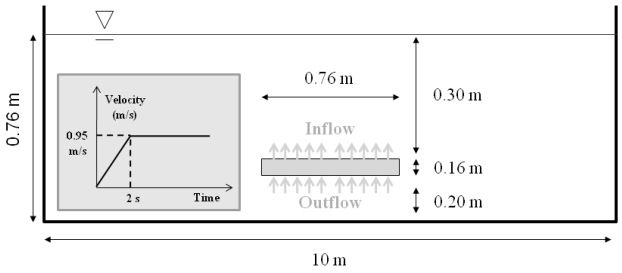

Figure 16 : Ideal case of simulation

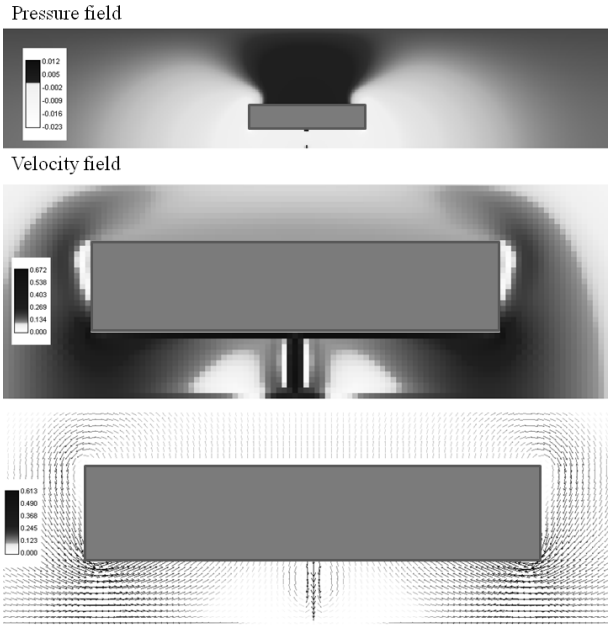

Figure 17 : Pressure and Velocity fields after 2s

The new module is applied hereafter for an ideal case that outlines the effect of both the bottom ground

and of the rigid sheet acceleration on both the fluid velocity field and the pressure distribution on the panel. This one is placed 20cm above the concrete ground and is supposed fixed. From the upper side of the panel enters an increasing inflow (from 0m/s up to 0.95m/s in 2s). From the lower side is extracted the same flow rate (see Figure 16).

The numerical simulation gives the velocity field and the hydrodynamic pressure field for the whole computational area (see Figure 17). Analyzing the velocity field clearly shows the apparition of vortices at the edges of the panel and in the central part behind the panel. The flow dynamic is clear.

In terms of pressure on the upper face, the values given in table 1 underline that the acceleration creates an increase in pressure. However, these values are lower than the ones recorded experimentally. This observation confirms that part of the hydrodynamic pressure created on the upper face is linked to the free surface. For the lower face, we observe bigger values close to the ones recorded experimentally. This proves the impact of the bottom ground.

Table 1 : Numerical pressure at gauges positions

	Central gauge	Lateral gauge
	[mm H²O]	[mm H²O]
Upper face	1.39	0.87
Lower face	6.88	6.02

6. CONCLUSION.

As explained in the introduction, the authors propose in this paper a contribution to the understanding and modelling of free surface flow induced by bodies upward. The study includes an overall analysis of the pressure field induced on the body. Reader would remind himself the study was motivated by the cost and the lack of flexibility of traditional physical models, as well as the weakness of the general knowledge about this complex phenomenon. Eventually, the experimental campaign, mainly focused on the vertical uplifting of a rigid sheet, has lead to the following contributions.

First, the six mechanisms identified and described in paragraph 4.4 give some basis to understand and predict the fluid behaviour and the fluid-structure interaction. In particular, evidence exposed before suggest the free surface plays an active role in the creation of the pressure field. The fourth mechanism, involving the fluid inertia, becomes insignificant far away from the free surface. The same conclusion applies to the sixth mechanism, involving free surface waves.

Second, the development of a vertical 2D module of WOLF supplied in information and validation cases along this research.

In conclusion, further research is needed to achieve a whole understanding of the behaviour of a body in motion in a free surface fluid. It would be interesting to repeat a similar experimental analysis for complex motion and/or complex body geometry.

7. REFERENCES.

[1.]Archambeau P., *Contribution à la modélisation de la genèse et de la propagation des crues et inondations,*, in *Applied Hydrodynamics and Hydraulic Constructions, PhD Thesis,* 2006, University of Liège.

[2.]Candel S., *Mécanique des fluides*, ed. Dunod. Vol. 1-2. 1990, Paris.

[3.]Canor A., *Analyse expérimentale des effets induits par le mouvement de redressement d'une porte basculante*, Master thesis, 2006, University of Liège.

[4.]Detrembleur S. and al., *An Explicit Projection Method for Solving Incompressible Navier-Stokes Equations*, Proceedings of the International Junior Researcher and Engineer Workshop on Hydraulic Structures IJREWHS'08, PISA, 2008.

[5.]Dewals B.J., *Une approche unifié pour la modélisation d'écoulements à surface libre, de leur effet érosif sur une structure et de leur intéraction avec divers constituants*, in *Applied Hydrodynamics and Hydraulic Constructions*, 2006, PhD Thesis, University of Liège.

[6.]Dewals B.J. and al., Depth-Integrated Flow Modelling Taking into Account Bottom Curvature, Journal of Hydraulic Research, 2006, 44(6), 787-795.

[7.]Erpicum S., *Optimisation objective des paramètres en écoulements turbulents à surface libre sur maillage multibloc*, 2006, PhD thesis, University of Liège.

[8.]Erpicum S. and al, *Interactions between numerical and physical modelling for the design and optimization of hydraulic structures - Example of a large hydroelectric complex*. in *International Symposium on Hydraulic Structures, XXII Congreso Latinoamericano de Hidráhulica*. 2006. Ciudad Guayana, Venezuela.

[9.]Kerger, F., *Analyse expérimentale des effets induits par le mouvement de redressement d'une porte basculante*, 2007, Master thesis, University of Liège.

[10.]Kochin, N.E., I.A. Kibel, and N.V. Roze, *Theoretical Hydromechanics*, ed. J.W.a.S. Ltd. 1964, New-York: Interscience Publishers.

[11.] Lazaro, P., et al., New Spillway at the Esch-sur-Sûre Dam, WasserWirtschaft, 2007, 10/2007, 42-44.

[12.] Wickert, G. and G. Schmausser, *Stahlwasserbau*, ed. Springer-Verlag. 1971, Berlin-Heidelberg-New York.